**Supplementary material for**
**Cannabidiol converts $NF_{\kappa}B$ into a tumor-suppressor in glioblastoma with defined antioxidative properties.**

Marie N. M. Volmar, Jiying Cheng, Haitham Alenezi, Sven Richter, Alisha Haug, Zonera Hassan, Maria Goldberg, Yuping Li, Mengzhuo Hou, Christel Herold-Mende, Cecile L. Maire, Katrin Lamszus, Charlotte Flüh, Janka Held-Feindt, Gaetano Gargiulo, Geoffrey J. Topping, Franz Schilling, Dieter Saur, Günter Schneider, Michael Synowitz, Joel A. Schick, Roland E. Kälin[1], Rainer Glass[1,*]

**Overview on Supplementary material:**

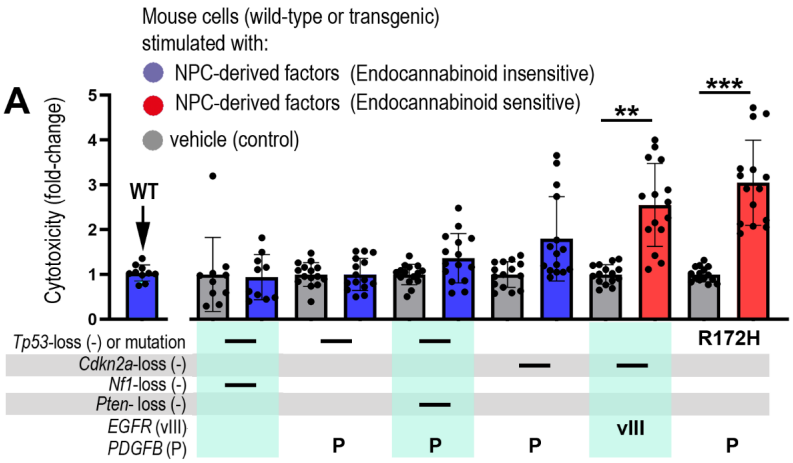
A
Mouse cells (wild-type or transgenic)
stimulated with:
NPC-derived factors (Endocannabinoid insensitive)
NPC-derived factors (Endocannabinoid sensitive)
vehicle (control)
Cytotoxicity (fold-change)
WT
**
***
Tp53-loss (-) or mutation
Cdkn2a-loss (-)
Nf1-loss (-)
Pten- loss (-)
EGFR (vIII)
PDGFB (P)
R172H
vIII
P
P
P
P

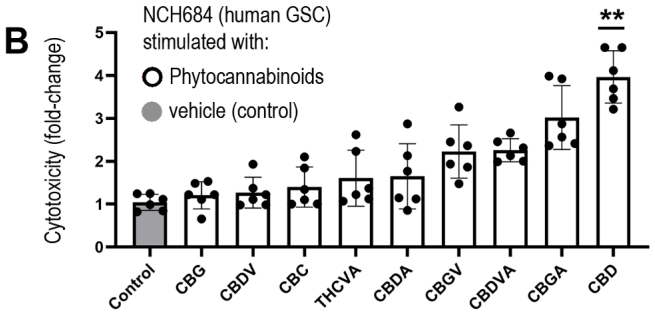
B
NCH684 (human GSC)
stimulated with:
Phytocannabinoids
vehicle (control)
Cytotoxicity (fold-change)
**
Control
CBG
CBDV
CBC
THCVA
CBDA
CBGV
CBDVA
CBGA
CBD

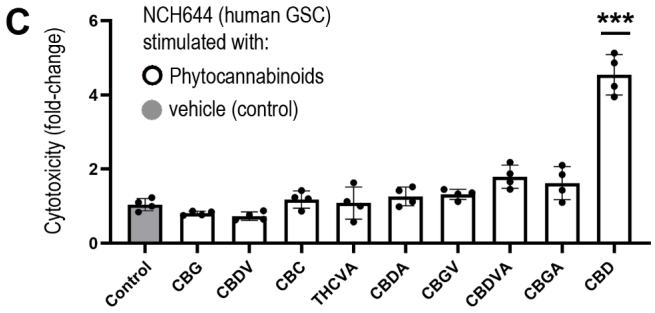
C
NCH644 (human GSC)
stimulated with:
Phytocannabinoids
vehicle (control)
Cytotoxicity (fold-change)
***
Control
CBG
CBDV
CBC
THCVA
CBDA
CBGV
CBDVA
CBGA
CBD

**Supplementary Figure 1. Endocannabinoid- and phytocannabinoid-sensitivity of brain tumor cells.** (**A**) Mouse transgenic glioma with different combinations of genetic driver mutations were established: Transgenic glioma harbored *Tp53* point-mutations or ablation of *Tp53*, *Cdkn2a, Pten* or *Nf1* (indicated by "-"), overexpression of PDGFRB (P) or mutant EGFR (vIII); cytotoxicity (fold-change) of transgenic glioma cells induced by neural precursor cell (NPC) released factors (NPC-conditioned medium containing endocannabinoids) was quantified; wild-type (WT) NPCs were used as controls. (**B**) Human, primary, stem-like glioblastoma cells (hGSC; named NCH684) were exposed to vehicle (0.01% DMSO) or stimulated with a range of non-psychotropic phytocannabinoids: Cannabigerol (CBG), Cannabidivarin (CBDV), Cannabichromene (CBC), Tetrahydrocannabivarinic Acid (THCVA), Cannabidiolic Acid (CBDA), Cannabigevarin (CBGV), Cannabidivarinic Acid (CBDVA) Cannabigerolic Acid (CBGA) or Cannabidiol (CBD) and cytotoxicity was quantified. (**C**) Human, primary, stem-like glioblastoma cells (hGSC; named NCH644) were exposed to vehicle (0.01% DMSO) or stimulated with a range of non-psychotropic phytocannabinoids (as in B) and cytotoxicity was quantified. Dots (in A - C) represent data from independent experiments; statistical significance in (A and D) was investigated by One-Way ANOVA with Bonferroni´s pair-wise comparison test (in A) or One-Way ANOVA with Tukey´s post-hoc test in B and C ($p<0.005$**; $p<0.001$***).

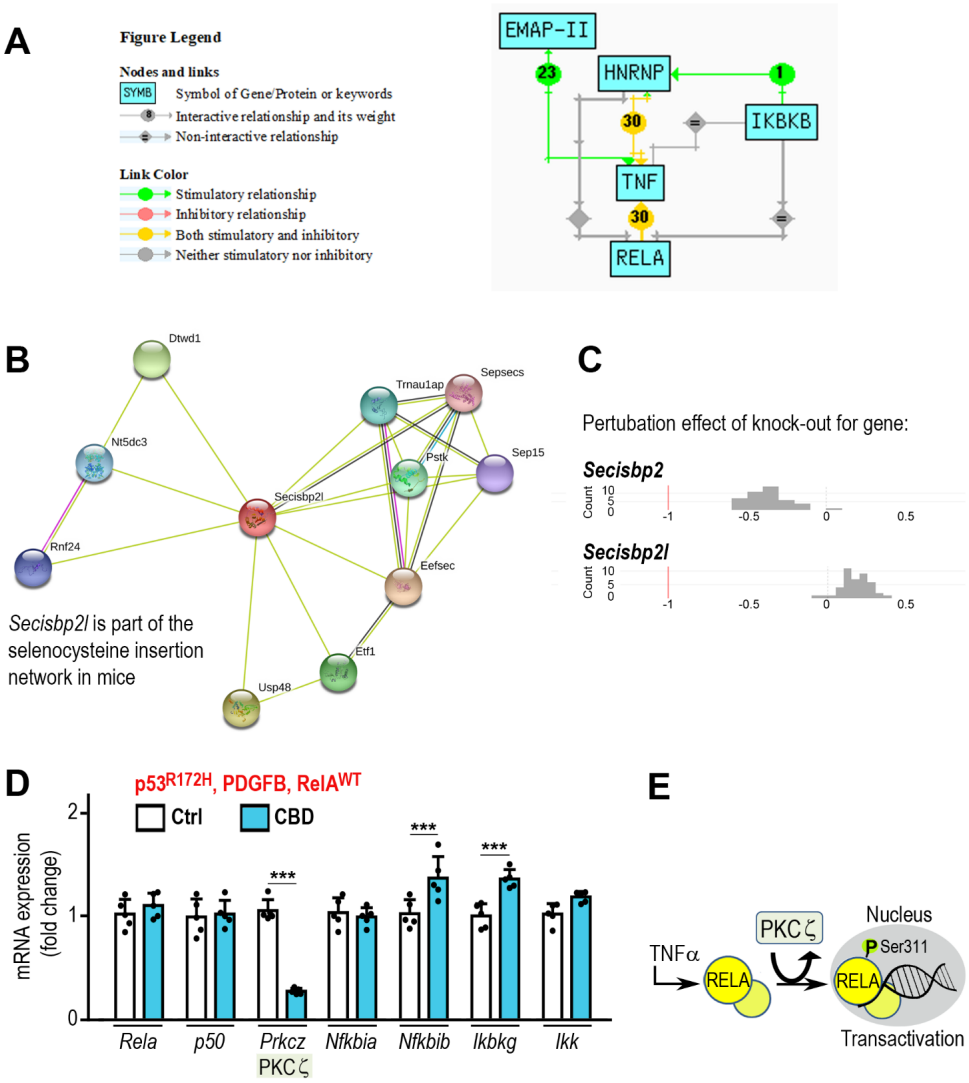
A
Figure Legend
Nodes and links
SYMB
Symbol of Gene/Protein or keywords
Interactive relationship and its weight
Non-interactive relationship
Link Color
Stimulatory relationship
Inhibitory relationship
Both stimulatory and inhibitory
Neither stimulatory nor inhibitory
EMAP-II
HNRNP
IKBKB
TNF
RELA
23
1
30
30
B
Dtwd1
Nt5dc3
Rnf24
Secisbp2l
Trnau1ap
Sepsecs
Pstk
Sep15
Eefsec
Etf1
Usp48
Secisbp2l is part of the selenocysteine insertion network in mice
C
Pertubation effect of knock-out for gene:
Secisbp2
Secisbp2l
Count
D
p53R172H, PDGFB, RelAWT
Ctrl
CBD
mRNA expression (fold change)
Rela
p50
Prkcz PKCζ
Nfkbia
Nfkbib
Ikbkg
Ikk
E
TNFα
RELA
PKCζ
Nucleus
P Ser311
Transactivation

**Supplementary Figure 2. Pharmacogenomics reveal a central role for NF$_\kappa$B and selenoproteins in CBD-induced hGSC cell-death. (A)** Knockouts (induced with a genome-wide CRISPR knockout-library in CBD-sensitive, CAS9-expressing *Tp53*$^{R172H}$, PDGFB tmBTCs) that were more than 10,000-fold enriched (as compared to vehicle-treated controls) in cells surviving CBD-application were identified (see supplemental table-1) and investigated by an algorithm for biological network reconstruction through text-mining (ChiliBot); permutations of pairwise searches suggested a role for three genes (*Emap-II*, *Hnrnp and Ikbkb*, identified by the pharmacogenomics-screen) in canonical (TNFα mediated) NF$_\kappa$B -signaling; integration of TNFα and the NF$_\kappa$B -subunit RelA together with the three identified genes in a gene-list query revealed the network-connections shown in (A). **(B)** The CRISPR-screen identified selenocysteine insertion sequence-binding protein 2-like (*Secisbp2l*) as a genetic ablation converting CBD-sensitive into CBD-insensitive tmBTCs (see supplemental table-2); *Secisbp2l* is part of the selenoprotein synthesis pathway in mice (participates in the selenocysteine-insertion pathway, as determined by interrogation of the STRING database). **(C)** The preponderant selenocysteine binding protein in humans is encoded by *SECISBP2*, but ablation of this gene (by CRIPR/Cas9-mediated knockout) is detrimental for cancer cell-viability, while loss of *SECISBP2L* is non-abrasive (numerical values reaching -0.5 or lower show cells do not tolerate a knockout, while positive values indicate tolerance, as observed DepMap database for CRISPR/Cas9 knockout studies); altogether, this can explain why *SECISBP2L* (but not *SECISBP2*) was found in our screen: *SECISBP2L*-knockouts are tolerable, but are predicted to have consequences for the synthesis of selenoproteins. **(D)** Q-PCR confirmed CBD-mediated downregulation of PKCζ (as compared to other genes of the NF$_\kappa$B -pathway). **(E)** Role of PKCζ in the canonical NF$_\kappa$B pathway: Inflammatory cytokines (TNF$\alpha$) initiate nuclear accumulation of RELA and simultaneous RELA-phosphorylation (on Ser311) by PKCζ, which is required for transactivation. Dots in (D) represent data from independent experiments; statistical significance (D) was investigated by One-Way-ANOVA plus Tukey post-hoc testing (***$p<0.001$).

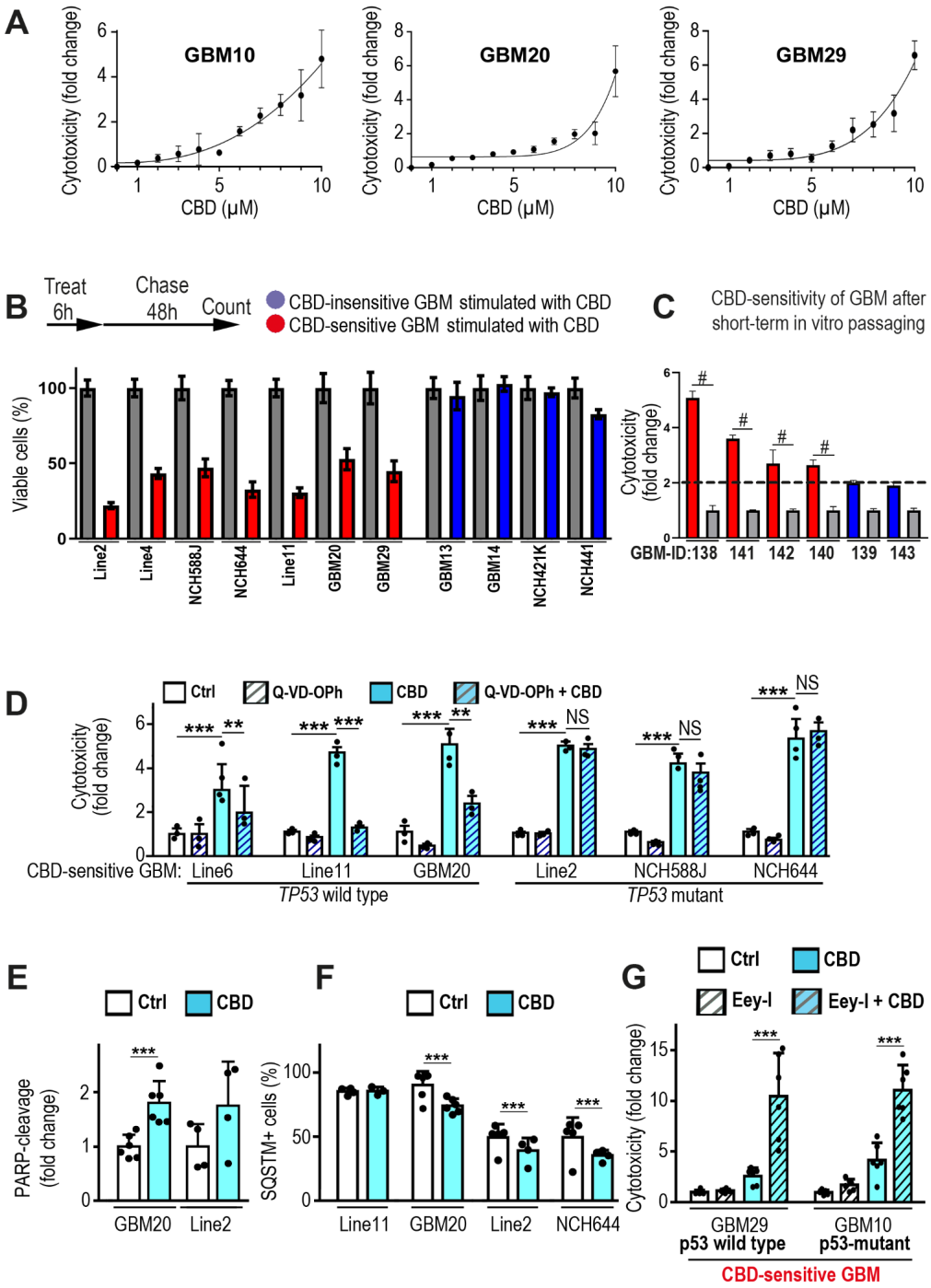
A
GBM10
GBM20
GBM29
Cytotoxicity (fold change)
CBD (µM)
B
Treat 6h
Chase 48h
Count
CBD-insensitive GBM stimulated with CBD
CBD-sensitive GBM stimulated with CBD
Viable cells (%)
Line2
Line4
NCH588J
NCH644
Line11
GBM20
GBM29
GBM13
GBM14
NCH421K
NCH441
C
CBD-sensitivity of GBM after short-term in vitro passaging
Cytotoxicity (fold change)
GBM-ID:138
141
142
140
139
143
D
Ctrl
Q-VD-OPh
CBD
Q-VD-OPh + CBD
Cytotoxicity (fold change)
CBD-sensitive GBM:
Line6
Line11
GBM20
Line2
NCH588J
NCH644
TP53 wild type
TP53 mutant
E
Ctrl
CBD
PARP-cleavage (fold change)
GBM20
Line2
F
Ctrl
CBD
SQSTM+ cells (%)
Line11
GBM20
Line2
NCH644
G
Ctrl
CBD
Eey-I
Eey-I + CBD
Cytotoxicity (fold change)
GBM29
p53 wild type
GBM10
p53-mutant
CBD-sensitive GBM

**Supplementary Figure 3. Cell-death in CBD-treated hGSC is executed by apoptosis or non-apoptotic pathways. (A)** CBD-induced cell-death in human stem-like glioblastoma cells (hGSC) named GBM10, GBM20 or GBM29 was quantified in a cytotoxicity assay over a concentration range; cytotoxicity is shown as fold-change versus vehicle control (0.01% DMSO); robust hGSC-death (more than 2fold change) was obtained with ≥ 8 µM CBD. **(B)** Effects of short CBD-pulses were investigated by counting hGSC under control conditions (grey bars) or after CBD application (10 µM CBD for 6 h; CBD-sensitive cells: red-bars; CBD-insensitive cells: blue-bars), 48 h after stimulation (control or CBD) viable cells were quantified; note that pulsed CBD application strongly attenuated the number of viable CBD-sensitive hGSC (but spared CBD-insensitive cells). **(C)** Biopsies from high-grade astrocytomas were maintained for very short time in vitro (tumors 139, 142 and 143 for three passages, tumor 140 for 4 passages and tumors 138 or 141 for 6 respectively 7 passages), CBD (or vehicle; controls) was applied as described and cytotoxicity was quantified (n=3 measurements); statistically significant induction of GBM-death by a factor of 2 or more (corresponding to a strong reduction in overall GBM cell viability, as shown in B) is indicated (#). **(D)** To determine if CBD-induced hGSC-death is executed via apoptosis we co-applied the pan-Caspase inhibitor Q-VD-Oph together with CBD and determined cytotoxicity as compared to negative (vehicle or Q-VD-Oph alone) and positive controls (CBD alone). CBD-mediated cell-death was corroborated in all CBD-sensitive hGSC; note that Q-VD-Oph efficiently blocked cell-death in a subset of p53 wild-type hGSC. **(E)** CBD-sensitive hGSC were exposed to CBD or vehicle (control; Ctrl), stained with an antibody specific for cleaved Poly-ADP-ribose-Polymerase (PARP) and inspected by flow cytometry; fractions of cells immunopositive for cleaved PARP were quantified, controls were arbitrarily defined as “1” and CBD-stimulated samples are shown as fold change relative to controls. **(F)** CBD-sensitive hGSC were stimulated with CBD or vehicle (control), stained with an antibody for p62 / sequestosome-1 (SQSTM) and fractions of cells immunopositive were quantified FACS, controls were arbitrarily defined as “1” and CBD-stimulated samples are shown as fold change relative to controls. **(G)** CBD-sensitive hGSC were incubated with vehicle (control), the ER-stress inducer Eeyarestatin-I (Eey-I; at a non-toxic concentration), CBD and combined CBD+Eey-I; note that Eey-I and CBD cooperatively induce hGSC cell-death (as determined by quantification of cytotoxicity). Statistical significance was investigated by One-Way ANOVA with Bonferroni´s pair-wise comparison test (NS = not significant, * $p<0.05$; ** $p<0.005$; *** $p<0.001$).

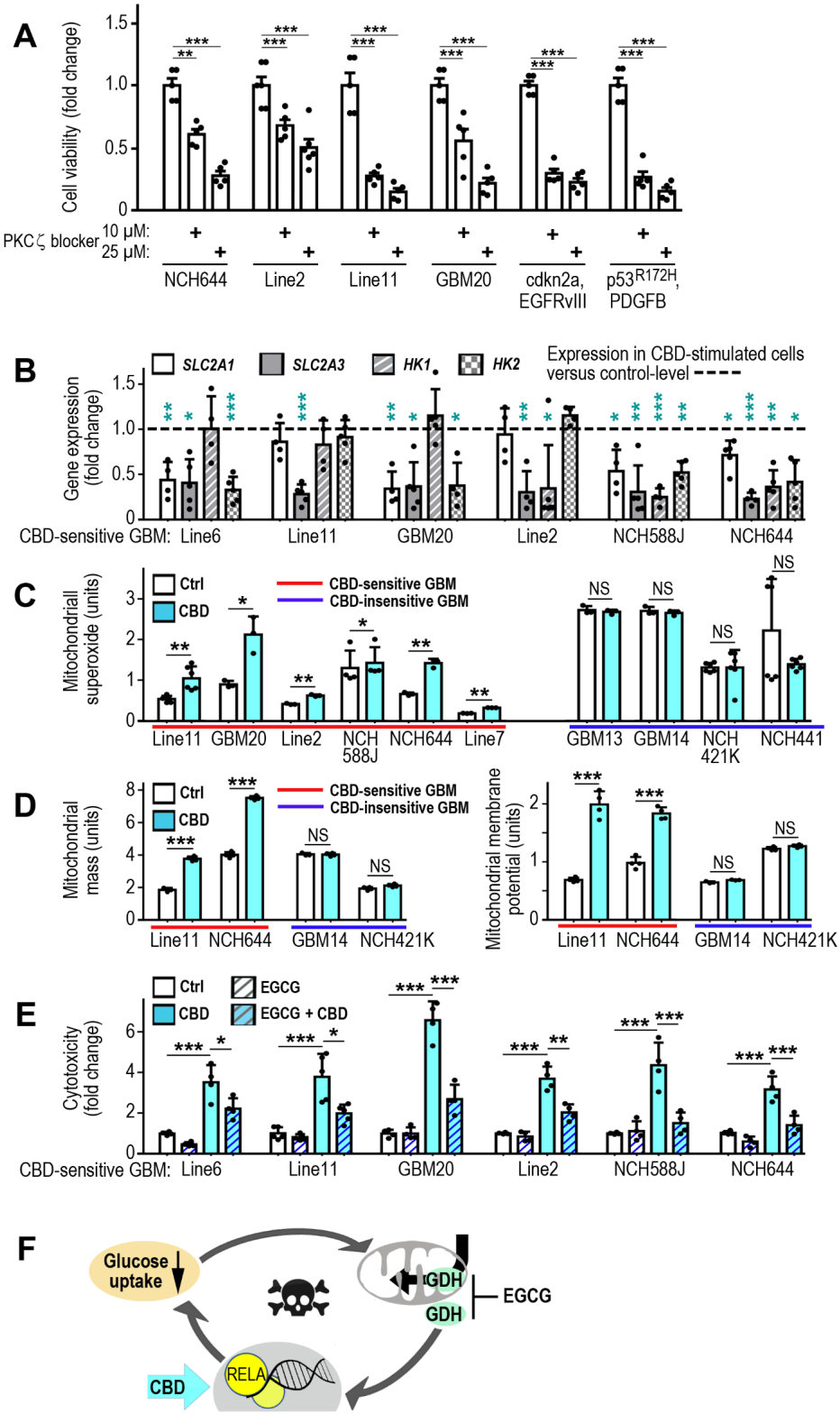
A
Cell viability (fold change)
PKCζ blocker
10 μM:
25 μM:
NCH644
Line2
Line11
GBM20
cdkn2a, EGFRvIII
p53R172H, PDGFB
B
SLC2A1
SLC2A3
HK1
HK2
Expression in CBD-stimulated cells versus control-level
Gene expression (fold change)
CBD-sensitive GBM: Line6
Line11
GBM20
Line2
NCH588J
NCH644
C
Mitochondriall superoxide (units)
Ctrl
CBD
CBD-sensitive GBM
CBD-insensitive GBM
Line11
GBM20
Line2
NCH 588J
NCH644
Line7
GBM13
GBM14
NCH 421K
NCH441
D
Mitochondrial mass (units)
Mitochondrial membrane potential (units)
Line11
NCH644
GBM14
NCH421K
E
Cytotoxicity (fold change)
EGCG
EGCG + CBD
CBD-sensitive GBM: Line6
Line11
GBM20
Line2
NCH588J
NCH644
F
Glucose uptake
GDH
EGCG
CBD
RELA

**Supplementary Figure 4. CBD-induced shifts in hGSC-metabolic cues are required for cell-death execution. (A)** Viability of CBD-sensitive human or mouse GBM cells was reduced by PKCζ-inhibition (in a dose-dependent manner). **(B)** Expression levels of key molecules for glucose uptake (SLC2A1, SLC2A3, HK1 and HK2) were determined by quantitative PCR under control conditions (arbitrarily set as "1", shown as dotted line) and after CBD-stimulation (fold-change from controls). **(C)** Mitochondrial-superoxide (SOX); **(D)** mitochondrial-mass, and -membrane-potential **(**MMP**)** were determined in a range of CBD-sensitive and –insensitive hGSC with or without CBD-application. The CBD-insensitive hGSC did not undergo any CBD-induced changes in mitochondrial physiology while CBD-sensitive tumor cells showed a profound increase in mitochondrial-SOX, -mass and –MMP (as compared to vehicle controls). **(E)** The glutamate dehydrogenase inhibitor EGCG largely abrogated CBD-induced hGSC-death. **(F)** Proposed model for glutamate dehydrogenase (GDH) and RELA in a feed-forward cycle for CBD-induced hGSC-cytotoxicity: CBD-attenuated glucose-uptake (A) necessitates metabolic adaption (B and C) through GDH (D), which is well established to promote nuclear localization of RELA under low glucose conditions (thereby spurring on nuclear accumulation of RELA lacking phosphorylation on Ser311). Statistical significance was investigated by One-Way-ANOVA with Bonferroni´s pair-wise comparison test (NS = not significant, * $p<0.05$; ** $p<0.005$; *** $p<0.001$).

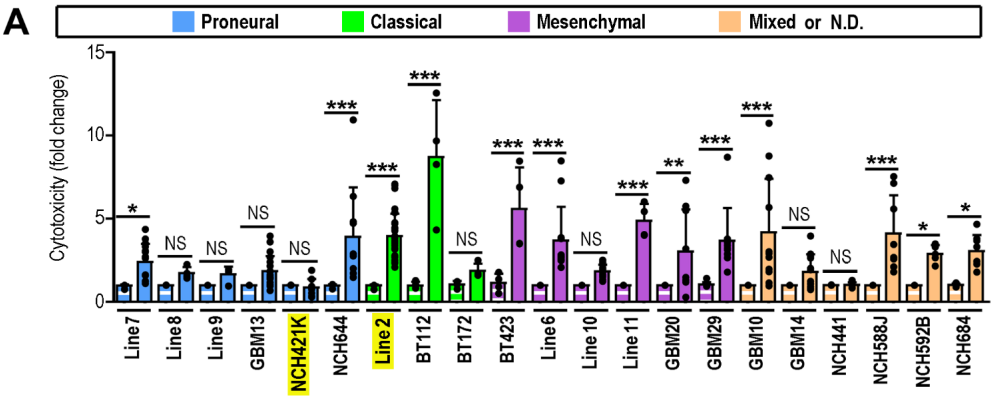
A
Proneural
Classical
Mesenchymal
Mixed or N.D.
Cytotoxicity (fold change)
15
10
5
0
*
NS
NS
NS
NS
***
***
***
NS
***
***
NS
***
**
***
***
NS
NS
NS
***
*
*
Line7
Line8
Line9
GBM13
NCH421K
NCH644
Line 2
BT112
BT172
BT423
Line6
Line 10
Line 11
GBM20
GBM29
GBM10
GBM14
NCH441
NCH588J
NCH592B
NCH684

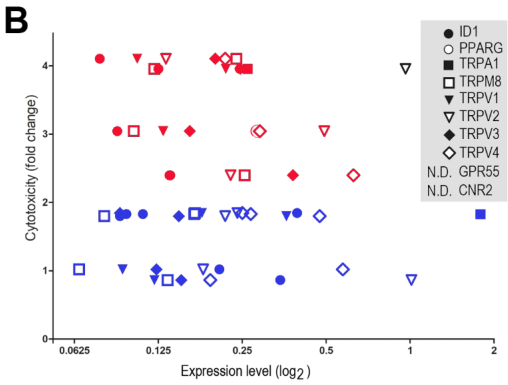
B
Cytotoxicity (fold change)
Expression level (log2)
0.0625
0.125
0.25
0.5
1
2
ID1
PPARG
TRPA1
TRPM8
TRPV1
TRPV2
TRPV3
TRPV4
N.D. GPR55
N.D. CNR2

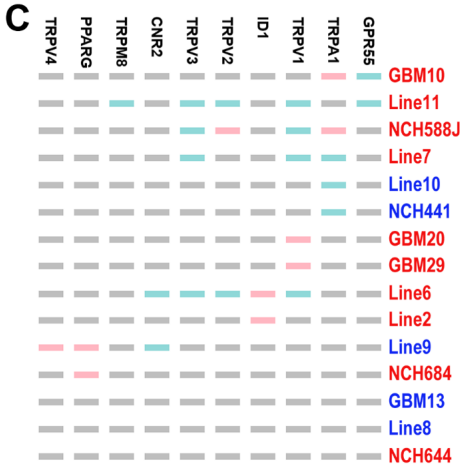
C
TRPV4
PPARG
TRPM8
CNR2
TRPV3
TRPV2
ID1
TRPV1
TRPA1
GPR55
GBM10
Line11
NCH588J
Line7
Line10
NCH441
GBM20
GBM29
Line6
Line2
Line9
NCH684
GBM13
Line8
NCH644

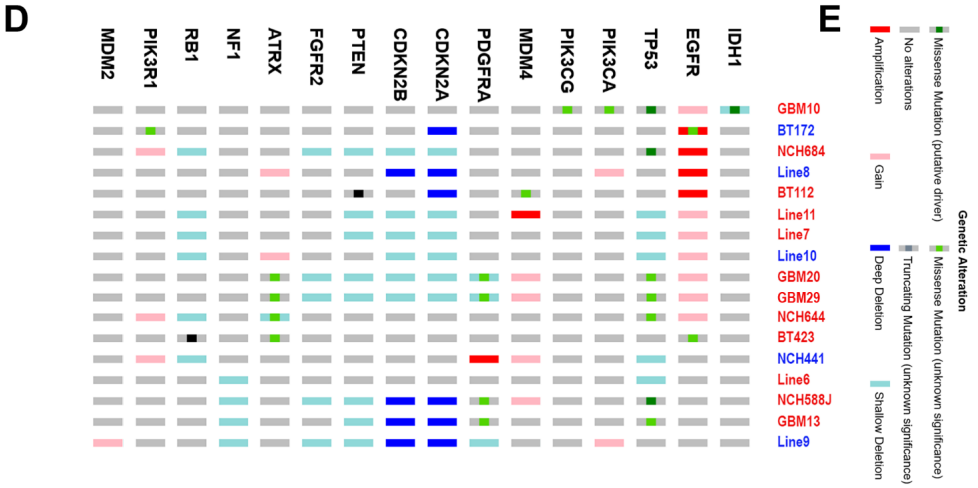
D
MDM2
PIK3R1
RB1
NF1
ATRX
FGFR2
PTEN
CDKN2B
CDKN2A
PDGFRA
MDM4
PIK3CG
PIK3CA
TP53
EGFR
IDH1
GBM10
BT172
NCH684
Line8
BT112
Line11
Line7
Line10
GBM20
GBM29
NCH644
BT423
NCH441
Line6
NCH588J
GBM13
Line9
E
Amplification
Gain
Deep Deletion
Shallow Deletion
No alterations
Truncating Mutation (unknown significance)
Missense Mutation (putative driver)
Missense Mutation (unknown significance)
Genetic Alteration

**Supplementary Figure 5. CBD-sensitivity of hGSC is not predicted by established markers for GBM-subsets or phytovanilloid signaling. (A)** Human primary hGSC were grouped according to GBM-subtypes (color-coded as proneural, classical or mesenchymal ; "mixed" comprises GBM previously designated as "neural"; N.D., not determined as exhibited in Supplemental Table-1), treated as described in Figure-1a (maintained under control conditions or treated with CBD); after 48 h cytotoxicity was quantified: Controls (bars with white pattern) were arbitrarily set as "1" and fold-change of CBD-induced cytotoxicity (as compared to controls) is indicated; note that CBD-sensitivity has no stringent relation with GBM-subtypes. **(B)** CBD-induced cell-death was previously related to activation or inhibition of different receptors or the transcription factor ID1; expression levels for these molecules were determined by qPCR (see list of symbols for each gene; log2 expression levels are presented; ND = not detected) and related to the cytotoxicity observed after CBD-application (symbols for CBD-sensitive hGSC in red, CBD-insensitive hGSC in blue); note that there is no correlation of expression-levels with CBD-sensitivity. **(C)** Copy number alterations (as determined by SNP-arrays) for genes listed in (B) or for known driver-mutations of human GBM **(D)** were inspected in CBD-sensitive (red) or CBD-insensitive hGSC (blue); note that there are no copy-number alterations that are specifically enriched in CBD-sensitive / insensitive hGSC; visualized by OncoPrint from cBioPortal with the symbols specified in **(E).**

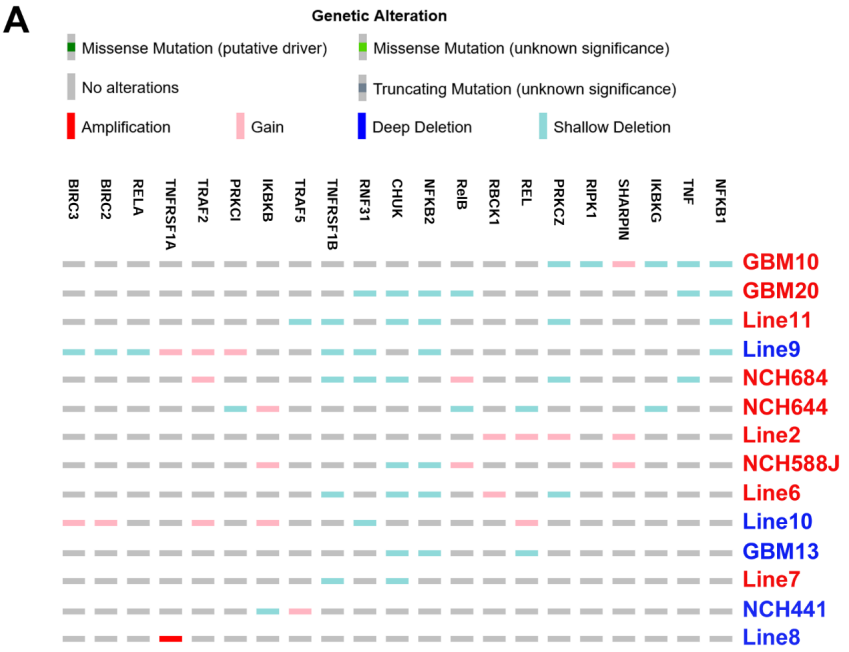
A
Genetic Alteration
Missense Mutation (putative driver)
Missense Mutation (unknown significance)
No alterations
Truncating Mutation (unknown significance)
Amplification
Gain
Deep Deletion
Shallow Deletion
BIRC3
BIRC2
RELA
TNFRSF1A
TRAF2
PRKCI
IKBKB
TRAF5
TNFRSF1B
RNF31
CHUK
NFKB2
RelB
RBCK1
REL
PRKCZ
RIPK1
SHARPIN
IKBKG
TNF
NFKB1
GBM10
GBM20
Line11
Line9
NCH684
NCH644
Line2
NCH588J
Line6
Line10
GBM13
Line7
NCH441
Line8

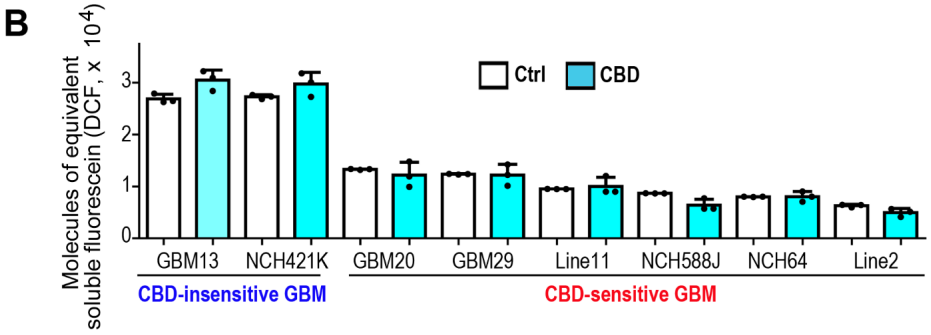
B
Molecules of equivalent soluble fluorescein (DCF, x 10^4)
0
1
2
3
Ctrl
CBD
GBM13
NCH421K
GBM20
GBM29
Line11
NCH588J
NCH64
Line2
CBD-insensitive GBM
CBD-sensitive GBM

**Supplementary Figure 6. Low ROS-levels are restricted to CBD-sensitive hGSC, while genetic alterations of NFκB-pathway components are shallow and non-discriminatory.** **(A)** A set of 22 genes representing the core of the canonical NF-κB pathway were investigated for copy-number alterations present in hGSC cells used in this study (data for 21 genes are shown, the gene *CYLD* was never altered and is therefore absent from the list), data were visualized by OncoPrint, symbols (Genetic Alteration) indicate presence / absence of mutations; note that there were no genetic alterations specifically enriched in CBD-sensitive / insensitive hGSC (interrogation of the TCGA-database for GBM confirmed that point-mutations for these genes were extremely rare: Missense mutations of unknown significance occurred only in a total of 10 samples, out of 257 samples; no sample contained more than one mutation). **(B)** Flow cytometry was used to determine soluble equivalent of fluorescein (MESF) for H2DCFDA (providing a quantitative assessment for reactive oxygen species; ROS) in a panel of CBD-sensitive or -insensitive hGSC before and after CBD-application.

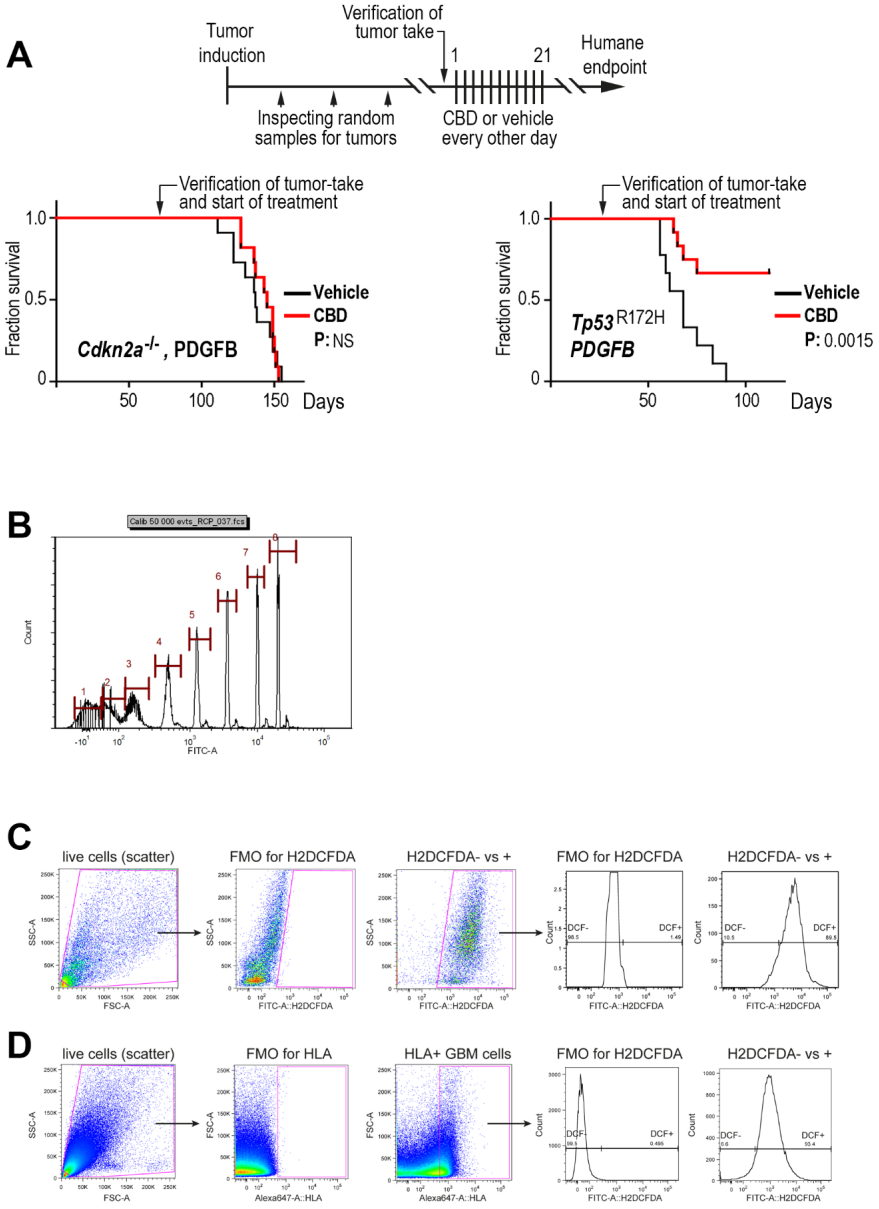
A
Tumor induction
Verification of tumor take
1
21
Humane endpoint
Inspecting random samples for tumors
CBD or vehicle every other day
Verification of tumor-take and start of treatment
Fraction survival
Cdkn2a-/-, PDGFB
Vehicle
CBD
P: NS
Days
Tp53 R172H
PDGFB
P: 0.0015
B
Count
FITC-A
C
live cells (scatter)
FMO for H2DCFDA
H2DCFDA- vs +
SSC-A
FSC-A
FITC-A::H2DCFDA
DCF-
DCF+
D
FMO for HLA
HLA+ GBM cells
Alexa647-A::HLA

**Supplementary Figure 7. CBD-mediated therapeutic effects in immunocompetent models and calibration for flow cytometry. (A)** CBD-mediated therapeutic effects were tested in two orthotopic, transgenic models corresponding to tmBTC characterized in vitro as CBD-sensitive or -insensitive; in a first step we induced GBM in transgenic mouse lines (cdkn2a-knockout mice or animals containing cre-inducible alleles for the Tp53 gain of function mutation R172H) by infusion (into the subventricular zone) of a vector inducing the expression of PDGFB and cre-recombinase; subsequently, randomly selected mice were inspected for GBM growth; when tumor-take was confirmed pharmacological treatment (CBD or vehicle) was performed and overall survival (until a pre-defined humane endpoint) was monitored (summarized in a schematic); note that CBD-treatment (red-lines) of established tumors prolonged survival (as compared to controls; blue lines) specifically in gliomas that were identified as CBD-sensitive in vitro ($p53^{R172H}$, PDGFB). **(B)** Bead calibration used for FACS-instrument settings to determine equivalents of soluble fluorescein (for 2',7'-dichlorodihydrofluorescein diacetate, H2DCFDA, measurement). **(C)** Cultivated hGSC cells were investigated for H2DCFDA-generated fluorescence by flow cytometry: The analysis was restricted to single, viable cells with sound fluorescence signals (as compared to negative controls; FMO) for oxidized H2DCFDA. **(D)** hGSC were excised from mouse brains, separated into single-cell suspensions, immunostained for human MHC (HLA, visualized with Alexa-647) and incubated with H2DCFDA, cells were investigated for fluorescent (oxidized) H2DCFDA and for Alexa-647 (immunofluorescence) by flow cytometry: The analysis was restricted to single, viable cells with sound fluorescence signals (as compared to negative controls; FMO) for Alexa-647 and with reliable detection for H2DCFDA (as compared to negative controls; FMO).

## MATERIALS AND METHODS

### Cell culture

Biopsies from human primary and recurrent hGSC were obtained from planned resections (approval was obtained from the ethics committee of Charité university clinics, license numbers EA112/2001, EA3/023/06 and EA2/101/08 and from the university clinics Kiel, license number D-408-14 and D-562-15; for primary cell cultures obtained from high-grade astrocytomas referenced in supplemental table-3) and cultured under neurosphere conditions at 37°C in a humidified atmosphere of 5% CO2; in cell-culture media previously established to maintain stem-like properties (see Supplemental table-1 for specification and references): DMEM/F12 containing B27 cell-culture supplement and EGF, FGF (both at 10 ng/ml; GBM10, GBM13, GBM14, GBM20, GBM29, BT112, BT172, BT423) or in NeuroCult basal medium containing NeuroCult proliferation supplement and EGF, FGF (both at 10 ng/ml; for Line2, Line6, Line7, Line8, Line9, Line10, Line11, NCH441, NCH421K, NCH588J, NCH592B, NCH644, NCH684). Cells were passaged 3 times per week using a seeding density of 0,3-0,5x $10^6$ cells/10ml. Tumorigenic capacity of hGSC cells was determined after orthotopic implantation. Mycoplasma were regularly tested and affected cells were discarded. Drugs were applied at concentrations indicated in the text and were diluted into DMSO (final concentration of DMSO was 0.01%); consequently we used 0.01% DMSO as vehicle solution. Biopsies from high-grade astrocytomas were freed from blood vessels, connective tissue and meninges as far as possible, dissociated mechanically in Dulbecco's modified Eagle's medium (DMEM; Thermo Fisher Scientific, Waltham, MA, USA) plus 0.05% DNase plus 0.03% trypsin, cultured in DMEM supplemented with 10% fetal bovine serum (FBS; Thermo Fisher Scientific), 1% penicillin–streptomycin (10,000 U/ml; Thermo Fisher Scientific), and 2 mM additional L-glutamine (Thermo Fisher Scientific), and subcultivated every 2–4 weeks by trypsinization. Purity of the high-grade astrocytoma cells was ascertained by immunostaining with cell type specific

markers, and by the absence of contamination with mycoplasms. Tumors were diagnosed and classified according to WHO criteria by a pathologist.

ARRIVE guidelines were followed for all animal experiments. Permissions for animal experimentation were obtained from the local authorities (Regierung von Oberbayern) and all precuders were performed in accordance with local rules and regulations. Brains from C57/BL6 wild-type and transgenic mice were harvested at postnatal day 30 (P30), the subventricular zone (SVZ) was dissected, dissociated (using trypsin and collagenase), washed with DMEM-10% FCS and transferred into NPC culture medium (DMEM/F12 containing B27 supplement, EGF and FGF both at 10 ng/ml. Once neurosphere-formation was observed spheroids were triturated and expanded (until sphere size reached 200 – 250 µm). Neural stem and precursor cell capacity was verified by self-renewal capacity and by established multi-lineage differentiation paradigms (clonal plating, growth factor withdrawal and adherent cultivation on ornithine-laminin coated surface followed by immunofluorescence staining for neuronal and glial markers; see antibody-list) confirming that cultivated cells were bona fide NPCs. NPCs from transgenic mice were stably transfected or virally transduced with vectors for the expression of cre-recombinase, different proto-oncogenes (see vector-list) or both. Genetic manipulations were controlled by the expression of vector derived reporters (GFP or RFP), by PCR and/or Western-blotting.

**Genetic characterization of hGSC**

Genomic DNA (gDNA) and total RNA were isolated in parallel from samples (with sample-IDs indicated in supplemental table-1); DNA libraries were prepared using the TruSeq Custom Amplicon Low Input kit (Illumina, Inc.). Using the Illumina Design Studio (with hg19 as a refernce; targeted amplicon size of 250 bp) we generated an amplicon-based enrichment panel (TruSeq Custom Amplicon Low Input). With this approach we enriched for genes often exhibiting point-mutation in hGSC(27) (see table “amplicons”, below). Sequencing was

performed on the Illumina MiSeq sequencing system (Illumina Inc.; 2 x 250 bp paired-end). The resulting reads were quality controlled and mapped against the human reference genome (hg19). For all samples, sequence variations of the amplified regions of interest in comparison to the human reference sequence were identified and filtered based on reliability. Additionally, genome-wide copy number variation (CNV) profiles were analyzed from gDNA using the CytoScan assay in combination with a one-color based labeling and hybridization protocol. Signals on the CytoScan HD microarrays were detected using the Affymetrix GeneChip 3000 Scanner. Raw data were quality controlled and analyzed for copy number variations using the Affymet-rix ChAS software.

**Table: Amplicons analyzed in hGSC**

| Gene Symbol | Official Gene Name | Gene ID | Chromosome |
|---|---|---|---|
| *ATRX1* | Apicoplast-associated thioredoxin family protein | 546 | X |
| *EGFR* | Epidermal growth factor receptor | 1956 | 7 |
| *IDH1* | isocitrate dehydrogenase (NADP(+)) 1 | 3417 | 2 |
| *NF1* | neurofibromin 1 | 4763 | 17 |
| *PDGFRA* | platelet derived growth factor receptor alpha | 5156 | 4 |
| *PIK3CA* | phosphatidylinositol-4,5-bisphosphate 3-kinase catalytic subunit alpha | 5290 | 3 |
| *PIK3CG* | phosphatidylinositol-4,5-bisphosphate 3-kinase catalytic subunit gamma | 5294 | 7 |
| *PIK3R1* | phosphoinositide-3-kinase regulatory subunit 1 | 5295 | 5 |
| *PTEN* | phosphatase and tensin homolog | 5728 | 10 |

| | | | |
|---|---|---|---|
| *RB1* | RB transcriptional corepressor 1 | 5925 | 13 |
| *TP53* | tumor protein p53 | 7157 | 17 |

**Transgenic mouse models**

Transgenic mouse glioma models were obtained from mouse strains with germ-line or conditional knockouts for tumor suppressors deleted in hGSC(27), which were (partly) combined with conditional models for the deletion of *Rela* (p65)(48). All transgenic mouse strains were bred and raised at the animal facilities of the University Clinics Munich and the clinics of the Technical University Munich according to German law on animal welfare and approved by the "Regierung von Oberbayern" in Munich, Germany.

**Transgenic mouse strains**

| Strain | Source | Identifier | Reference |
|---|---|---|---|
| Ai9$^{(RCL\text{-}tdT)}$ | JaxLab | 007909 | Nat Neurosci. 2010, 13 (1): 133-40 |
| *Cdkn2A*$^{-/-}$ | NCI Frederick | Ink4A/Arf null (B6) | Cell. 1996, 5;85(1): 27-37 |
| *Tp53*$^{LSL.R172H}$ | JaxLab | 034620 | Cell. 2004, 119(6): 847-60 |
| *Tp53*$^{KO}$ | JaxLab | 002101 | Curr Biol. 1994, 4(1):1-7 |
| *Tp53*$^{LoxP}$ | JaxLab | 008462 | Genes Dev. 2000, 14(8): 994-1004 |

| | | | |
|---|---|---|---|
| Rela$^{tm1Rsch}$ | | MGI ID: 3713697 | J Clin Invest. 2007; 117(6):1490-501 |
| PTEN $^{flox}$ | JaxLab | 006440 | Genesis. 2002, 32(2): 148-9 |
| mT/mG, dual RFP / GFP reporter | JaxLab | 007676 | Genesis. 2007, 45 (9): 593-605. |
| Nf1$^{flox}$ | JaxLab | 017640 | Cell. 2011, 146(2):209-21 |

The genes encoding *Tp53* and *Nf1* are located on the same chromosome and linked *Tp53* and *Nf1d*ouble-transgenic mice were obtained (through crossing over events in meiosis) after several generations of breeding. Human GSC cells were orthotopically implanted into B6.129S6-Rag2$^{tm1Fwa}$ N12 (immunodeficient Rag2-KO) mice (purchased from Taconic).

**Plasmid transfection into mammalian cells**

Cells were seeded into serum- and antibiotics-free medium, 3µg of plasmid was mixed with OptiMem and Plus-reagent, then lipofectamine was added (all from Thermo Fisher Scientific), the mixture was incubated and subsequently applied to the plated cells. After 24 h cells were plated into selection medium (for stable transfection); selective agents were omitted during experiments.

**ORF-Sources for gene-expression constructs**

| ORF | Species | Provider | Identifier | Reference |
|---|---|---|---|---|

| | | | | |
|---|---|---|---|---|
| *TP53* | Human | Addgene | #69003 | Nucleic Acids Res. 2014, 42(12): 7666-80 |
| *TP53* | Mouse | Addgene | #12139 | J Cell Physiol. 1998, 177(2): 364-76 |
| *TP53V133A* | Human | Addgene | #16435 | Science. 1990, 249(4971):912-5 |
| *TP53R175H* | Mouse | Addgene | #14854 | Cell. 2004, 119(6):847-60 |
| *TP53R175H* | Human | Addgene | #16436 | Science. 1990, 249(4971):912-5 |
| *TP53R248W* | Human | Addgene | #16437 | Science. 1990, 249(4971):912-5 |
| *TP53R249S* | Human | Addgene | #16438 | Science. 1990, 249(4971):912-5 |
| *TP53R273H* | Human | Addgene | #16439 | Science. 1990, 249(4971):912-5 |
| *EGFR* | Human | Addgene | #44185 | Biochemistry. 2008, 47(39): 10314-23 |
| *EGFRvIII* | Human | Addgene | #20737 | Neuro Oncol. 2009, 11(1):9-21 |
| *PDGFB* | Human | Malatesta, P. | | Int J Cancer, 124 (2009) 2251-2259 |

ORFs for the expression of wild-type or mutant forms of *RelA* (mouse) were generated as synthetic gene (with NM_009045.5 as a template) and expressed in pcDNA3.1.

**Expression vectors**

| **Name** | **Type** | **Provider** | **Identifier / Cat.Nr.** | **Reference** (non-commercial providers) |
|---|---|---|---|---|
| pBABE-puro | RV | Addgene | #1764 | Nucleic Acids Res. 1990, 18(12): 3587-96. |
| pLenti6/V5-DEST | LV | Thermo Fisher Scientific | #V49610 | |
| pLVxIRES-ZsGreen1 | LV | Takara | #632187 | |
| pcDNA3.1 | Stable mammal. express. | Thermo Fisher Scientific | # V79020 | |
| pIRES2-EGF | Stable mammal. express. | Novo ProLab | # V11106 | |
| pNFkB-DD-ZsGreen1 | Mammal. reporter | Takara | #631080 | |

**Pantropic virus production and transduction**

Lentiviruses were generated using the Mission third generation lentiviral packaging system (Merck). HEK293T were plated co-transfected with packaging mix and transfer vector containing the gene of interest, 24 h later cells obtained fresh medium; lentiviral particles were harvested on day 2 and 3 post-transfection, filtered, aliquoted and stored at -80°C until

use. For in vivo applications VSV-G coated virus-particles were sedimented (concentrated) by ultra-centrifugation (200,000 g) and virus titers of 5x $10^9$ cfu (or higher) were obtained

**CRISPR/Cas9 screen**

Mouse glioma cells were infected with the genome-wide gRNA lentiviral library(49) (Addgene #50947) at an MOI of 0.3. Three days after infection, $3.5 \times 10^6$ BFP-positive cells were sorted and cultured for an additional 4 days. Then, transduced cells were split into two fractions of equal cell-number and treated with CBD or with vehicle (0.01% DMSO; controls) for 16 h. Then media were exchanged (to fresh medium without DMSO or CBD) and surviving cells were expanded for 6 days (separately in each experimental group). Genomic DNA was extracted and used for PCR templates. gRNA was amplified (Hot start PCR) using 15 ng of the whole-genome lentiviral plasmid library per reaction. The PCR products were purified with Agencourt AMPure XP beads in a PCR-product-to-bead ratio of 1:0.7. The purified libraries were quantified and sequenced on Illumina HiSeq2500 by 50-bp single-end sequencing (for the entire libraries gRNA sequences were extracted by removing constant regions from each read and these were used to count quantify and assign the number of reads of each gRNA in the library using Encore software(50).

**Transcriptomics**

Total RNA was isolated from cell-pellets using the RNeasy Mini Kit (Qiagen) according to the manufacturer's instructions including on-column DNase digestion; RNA concentration was determined (NanoDrop ND-1000 spectral photometer; Peqlab). High-quality total RNA samples (A260/A280 ratio ≥ 1.9; A260/A230 ratio ≥ 2.0) were used for subsequent steps of RNA quality control (2100 Bioanalyzer with RNA 6000 Nano and Pico LabChip Kits; Agilent Technologies) and samples with RIN values ≥9 were used for library preparation (TruSeq Stranded mRNA HT technology). Then, all samples were again quality controlled (DNA 1000 LabChip kits on the 2100 Bioanalyzer; Agilent Technologies). These samples showed a clear

and pure band at approximately 260 nt, DNA concentration was determined and the sequencing library was quantified (Qubit ds DNA HS Assay Kit ; Invitrogen). Sequencing of the library was performed at a final concentration of 1.8 pM and with a 1% PhiX v3 control library spike-in (Illumina) on the NextSeq500 sequencing system (Illumina). For cluster generation and sequencing of all samples, a high output single-end 75 cycles (1x75Bp SE) run was performed (NextSeq500). Sequencing was operated under the control of the NextSeq Control Software (NCS).

**Quantitative PCR**

RNA extraction and quality controls were performed as described above (transcriptomics). The High-Capacity cDNA Reverse Transcription Kit (Thermo Fisher Scientific) was used for reverse transcription of total RNA into single stranded cDNA with the aid of random hexamer primers according to the manufacturer's instructions. The cDNA samples were analyzed in triplicates; TaqMan Gene Expression Master Mix (Thermo Fisher Scientific) and the TaqMan assays indicated in table "PCR probes" were used for real-time PCR amplification. The amplifications were run in 384-well format on a ViiA7™ instrument (Thermo Fisher Scientific).

**PCR probes**

| Gene symbol | TaqMan assay ID | Gene symbol | TaqMan assay ID |
|---|---|---|---|
| *Ikbkg* | Mm00494927_m1 | *Prkcz* | Mm00776345_g1 |
| *Nfkbib* | Mm00456853_m1 | *Prkcq* | Mm00435802_mH |
| *Nfkbia* | Mm00477800_g1 | *Prkcd* | Mm00440884_g1 |
| *Ikk1* | Mm00432529_m1 | *Prkcb* | Mm00435749_m1 |
| *RelA* | Mm00501346_m1 | *Gapdh* | Mm99999915_g1 |
| *Nfkb2* | Mm00479807_m1 | *ActB* | Mm01205647_g1 |
| *Nfkb1* | Mm00476379_m1 | *IKBKG* | Mm00494927_m1 |
| *TRPA1* | Hs00175798_m1 | *TRPV4* | Hs01099348_m1 |
| *TRPV1* | Hs00218912_m1 | *TRPM8* | Hs01066596_m1 |
| *CNR2* | Hs00361490_m1 | *ACTB* | Hs01060665_g1 |
| *PPARG* | Hs01115513_m1 | *SLC2A1* | Hs00892681_m1 |
| *GAPDH* | Hs02758991_g1 | *SLC2A3* | Hs00359840_m1 |
| *ID1* | Hs00357821_g1 | *HK1* | Hs00175976_m1 |
| *GPR55* | Hs00995276_m1 | *HK2* | Hs00606086_m1 |
| *TRPV2* | Hs00901648_m1 | *TRPV3* | Hs00376854_m1 |

**In vitro cytotoxicity assay**

Cytotoxicity was detected using the CytoTox-Fluor™ cytotoxicity assay from Promega. In 96 well-plates, 3 x$10^3$ in 50µl (5 replicates per condition) were treated for 24 hours with 50µl of vehicle/drug in NPC medium without phenol red. 40µl of cells and diluted bis-AAF-R110 substrate (1:1 ratio) incubated for 2 hours before measuring fluorescence intensity in a InfiniteF200 fluorescence plate reader (Tecan; 485nm Ex / 520nm Em); blanks were subtracted from all wells and the fluorescence read-out for untreated cells (vehicle control) was normalized to 1. Read-outs from treated cells were normalized to those of untreated cells and fold change of relative cytotoxicity calculated for each well. Outliers were detected and omitted, if any, using the Grubbs test. Graphs were generated using the GraphPad Prism software version 5.01.

**In vitro viability and proliferation assays**

The CellTiter Non-radioactive Cell Proliferation Assay (Promega) was used according to manufacturer´s instructions. Cells were seeded and treated as in the cytotoxicity assay. After 48 hours of incubation at 37°C in a humidified atmosphere, each well incubated with 15µl of dye solution for 4 h at 37°C; 100µl of solubilization/stop solution was added to each well and incubated 1 hour at 37°C. The absorbance was then recorded using an absorbance plate reader set at 570nm (SoftmaxPro software). Blanks were subtracted from all wells and fold change to vehicle control was calculated. The CellTiter 96 AQueous Non-Radioactive Cell Proliferation Assay (Promega) was used according to manufacturer´s instructions. Cells were seeded and treated as in the MTT assay. After 72 h at 37°C in a humidified atmosphere, each well incubated with 20µl of MTS/PMS solution for 4 h at 37°C. To stop the reaction, 25µl of 10% SDS solution was added to each well and incubated 1 hour at 37°C. The absorbance was then recorded using an absorbance plate reader set at 490nm using the SoftmaxPro software. Blank was subtracted from all wells and fold change to vehicle control was calculated.

**Transcription factor binding array**

Transcription factor binding to cognate gene-promoter sequences was quantified with the ER Stress (UPR) TF Activation Profiling Plate array (Signosis; according to instructions), simultaneously indicating the DNA-binding activity of XBP-1, ATF4, ATF6, GADD153/CHOP, CBF/NFY, SREBP1, YY1, ERR, ATF3, AP-1, FOXO1, IRF, p53, NFκB and NRF2/ARE; hGSC cells were inspected over a time-course after vehicle-treatment (control) or after stimulation with 10 µM CBD; reproducible data were obtained after 20 h of treatment / control and fold-changes in DNA-binding of all TFs was calculated.

**Reporter-gene assay**

Patient-derived Glioblastoma cells were transfected with a reporter-construct encoding for the ProteoTuner™ Shield System N (Signosis; using lipofectamine, see above). Here, a destabilized form of GFP is expressed under a synthetic *RELA*-promoter (4x *PLAU*-promoter); in the presence of a cell-permeable compounds (Shield1) GFP is stabilized and accumulates inside the cell. This allows for active and controllable degradation of GFP and low background levels in reporter gene assays. Stable transfectants were used in all experiments. Green fluorescence was examined by fluorescence microscopy or flow cytometry; technical controls included addition of excessive Shield-1, which produced strong GFP conditions in all cells (serving as a positive control for hGSC cells without TNFα-inducible reporter-gene activity).

***In vivo* models**

Animal experiments were carried out in compliance with the German law on animal welfare, and all animal protocols were approved by the "Regierung von Oberbayern" in Munich, Germany. Mice were housed in standardized cages in the Walter Brendel Centre for Experimental Medicine, Ludwig-Maximilians-University (LMU) Munich, received chow ad libitum and were kept under a circadian rhythm with 12 h light and dark cycles in environmentally enriched conditions (max. 4 mice / cage).

To evaluate the capacity of the generated mouse gliomas to induce tumors *in vivo*, adult male and female mice (equal ratio; bred at the facility) were randomized, anesthetized and immobilized in flat-skull position in a stereotactic head holder. 0,1x $10^6$ cells/1 µl/mouse were inoculated using a 30-gauge Hamilton syringe approximately 1,5mm posterior and 1,5 mm lateral to the bregma. After operation, the skin was sutured, and mice placed back in their cage for recovery. The animals were inspected twice a day until humane end-point (when neurological symptoms occur that are firmly associated with end-stage disease). They were then anesthetized, perfused with PFA and their brain collected. Brains were placed in 30% sucrose for dehydration and cryopreserved in tissueTek O.C.T solution. Tumorigenesis was evaluated by hematoxylin-eosin staining, MR imaging and/or immunohistochemical staining.

For the induction of tumorigenicity in transgenic models concentrated virus particles were injected into the SVZ of young (P30) mice at the following stereotactic coordinates (using the bregma as a landmark): Antero-posterior +0.6 mm, medio-lateral 1.2 mm, dorso-ventral 1.2 mm. A volume of 0.5 µl concentrated virus-particles was infused (at a rate of 0.05 µl/ min) using an automated pump system. For in vivo CBD-application (drugs were applied in a fixed time-schedule) and Kaplan-Meier read-out immunodeficient mice were inoculated with hGSC or transgenic mice were infused with retroviral vectors (VSV-G pseudotyped) for the expression of proto-oncogenes. Tumorigenicity was determined by histological inspection of random samples from these cohorts of mice. After establishing tumor-growth mice were i.p. injected (every other day, for 21 days) with CBD (15mg/kg) or vehicle (5% Tween80, 5% ethanol in 0.9% saline).

**MRI screening**

For the MRI screening, mice were anesthetized with inhalation of isoflurane 2% (v/v) in an oxygen flow rate of 2 L/min. Imaging was performed on a 7 T small animal MR scanner (Agilent Discovery MR901 magnet and gradient system, Bruker AVANCE III HD electronics). A 72 mm dual-tuned 1H/13C birdcage resonator was used for radiofrequency transmission in combination with a two-channel fixed-housing mouse-brain surface-receiver array (Rapid Biomedical, Germany). T2-weighted images were acquired with a fast spin echo / rapid imaging with relaxation enhancement (RARE) sequence, with slice thickness 1 mm, field of view 20x20 cm, acquisition matrix 192x192, repetition time 2500 ms, effective echo time 40 ms, and fat-suppression enabled.

**Immunofluorescence**

Permeabilized cells were washed 3 times in 1x PBS. The primary antibodies incubated overnight at 4°C, washed 3 times with 1 x PBS and incubated in the dark for 2 hours at room temperature with a mixture of fluorescently labeled secondary antibody and Hoechst 33342 for nuclear counter-staining. Controls included e.g. omission of secondary antibody to exclude unspecific immunofluorescence-detection; quantification was performed using ImageJ providing data on fold-changes in time-course and pharmacological experiments: Nuclei (stained with DAPI) and RelA-immunofluorescence were visualized in separate channels, negative controls were used to define a detection-threshold for RelA and corrected total nuclear fluorescence (defined as the integrated density of fluorescence-staining of the nuclear region after background-subtraction) was obtained for each nucleus. Thereby we defined a first image-mask containing information on the size and position of all nuclei. Then we obtained a second mask containing results on specific RelA-staining. Both image-masks were overlayed and information on immunofluorescence for RelA (or phospho-RelA) in nuclear regions was automatically quantified.

**Primary antibodies**

| Antibody | Provider | Cat-Nr. | RRID |
|---|---|---|---|
| Rabbit anti NG2 | Millipore | AB5320 | AB_11213678 |
| Mouse anti- Polysialic-Acid- NCAM 60 | Millipore | MAB 5324 | AB_11210572 |
| Goat anti Doublecortin | SantaCruz | sc-271390 | AB_10610966 |
| Mouse anti Tuj1 | Sigma | T8578 | AB_1841228 |
| Mouse anti NeuN | Abcam | ab104224 | AB_10711040 |
| Rabbit anti GFAP | Abcam | ab7260 | AB_305808 |
| Mouse anti-S100ß | Sigma-Aldrich | S2532 | AB_477499 |
| Mouse anti-CNpase | Abcam | ab6319 | AB_2082593 |
| Rabbit anti Myelin Basic Protein | Abcam | ab40390 | AB_1141521 |
| Rabbit anti-Sox 2 | Abcam | ab97959 | AB_2341193 |
| Goat anti-Sox 2 | R&D Systems | AF2018 | AB_355110 |
| Rabbit anti-NFκB p65 Antibody | BioLegend | 622601 | AB_315955 |
| Rabbit anti-Phospho-NF-□B p65 (Ser311) | Thermo Fisher | PA5-37720 | AB_2554400 |
| Mouse anti-HLA-A,B,C Alexa Fluor-647 | Biolegend | 311414 | AB_493135 |
| Mouse anti-PARP1 (cleaved Asp214) - eFluor 450, | eBioscience | 48-6668-42 | AB_2574097 |

| | | | |
|---|---|---|---|
| Mouse anti-p62/SQSTM1 Alexa Fluor-647 | Novus Biologicals | Nbp2-23490af647 | Not available |
| Rabbit anti-phospho-MLKL (Ser358) Antibody Set | EMD-Millipore | 17-10400 | Not available |
| rabbit anti-NFKB phospo p65 | Thermofisher Scientific | PA5-37720 | AB_2554328 |
| Mouse-anti nuclear Matrix Protein p84 (clone 5E10) | GeneTex International | GTX70220 | AB_372637 |
| rabbit anti-NFKB p65 | Biolegend | 622602 | AB_315956 |

**Secondary antibodies and conjugated fluorophores**

| Antibody | Provider | Cat-Nr. | RRID |
|---|---|---|---|
| Biotynilated donkey anti mouse | Jackson Immuno Research | 715-065-151 | AB_2340785 |
| Alexa 488 donkey anti rabbit | Jackson Immuno Research | 711-545-152 | AB_2313584 |
| Alexa Fluor 594 donkey anti rabbit | Jackson Immuno Research | 711-585-152 | AB_2340621 |
| Alexa Fluor 594 donkey anti rat | Jackson Immuno Research | 712-585-150 | AB_2340688 |
| Alexa Fluor 594 donkey anti mouse | Jackson Immuno Research | 715-585-151 | AB_2340855 |
| Alexa 488 donkey anti goat | Jackson Immuno Research | 705-545-147 | AB_2336933 |

| | | | |
|---|---|---|---|
| Alexa 647 donkey anti rat | Jackson Immuno Research | 712-605-153 | AB_2340694 |
| Alexa 647 donkey anti goat | Jackson Immuno Research | 705-605-003 | AB_2340436 |
| Alexa Fluor 488 conj. Streptavidin | Jackson Immuno Research | 016-540-084 | AB_2337249 |
| HRP conj. anti-mouse | Bio Rad | 170-5046 | AB_11125757 |
| HRP conj. anti-rabbit | Bio Rad | 170-5047 | AB_11125753 |

**Western blotting**

SDS-PAGE was performed to assess nuclear localization and phosphorylation of NFKB. Nuclear/cytoplasm separation was performed using an NE-PER kit (#78833, Thermofisher Scientific). Protein concentration was determined using a Bradford protein assay kit (#500-0202, Quick Start Bradford Protein Assay Kit 2, Bio-Rad). Samples (30 µg of protein per lane) were denatured in Lämmli buffer (#1610737, Biorad), loaded onto 10% acrylamide gels (A3699; Merck) and proteins separated by SDS-PAGE at 150 V for 80 min. Separated proteins were transferred to a polyvinylidene fluoride (PVDF) membrane (BioRad) at 400mA for 70 min. Non-specific antibody sites were blocked with 5% milk powder for 60 min at room temperature. Membranes were probed with primary and (after extensive washing) secondary

antibodies (see tables). For protein size estimation, the precision plus protein WesternC standard was used in combination with Streptactin conjugate (1:3000; #1610376 and #1610381, Biorad). Blots were developed with Supersignal West Pico Plus Chemoluminescent substrate kit (#34578, Thermofisher Scientific) and images were recorded on a Hamamatsu ORCA-ER imager using the Wasabi Image software (Hamamatsu Photonics).

**Flow cytometry**

$10^6$ cells were exposed to different experimental paradigms, centrifuged, and washed once with 1xPBS; cells were stained with fluorescently labeled surface antibody in FACS buffer (PBS with 0.5% BSA and 2mM EDTA; 1µg antibody/ $10^6$ cells/ 100µl FACS buffer) for 30 minutes on ice in the dark; washed twice with FACS buffer, and transferred to FACS tubes for acquisition in a LSR Fortessa (Becton Dickinson). For detection of intracellular antigens cells were fixed for 20 minutes at RT, permeabilized, washed and incubated with staining solution (as above). Cells were always kept on ice, in the dark until flow cytometric acquisition. To quantify the relative amount of fluorescence molecules that corresponds to the acquired median fluorescence intensity (MFI), rainbow calibration particles (RCP) where acquired the same day and using the same laser settings as the samples. Exported fcs files were analyzed in FCS express5 (De Novo Software) for MFI and molecules of equivalent fluorescein (MEFL) using a standard curve with pre-defined RCP MEFL concentrations. The normalized median fluorescence intensity (nMFI) was also calculated by dividing the MFI by the number of events (MFI/number of events).

For *ex vivo* imaging of hGSC ROS levels immune-deficient mice bearing patient-derived hGSC xenografts were sacrificed and brains collected. The tumor was dissected, tumor biopsy cut into 10mg pieces, and mashed through a cell strainer. The cell suspension was stained with human HLA A, B, C-AlexaFluor647 and 20µM H2DCFDA in 1x PBS for 30 minutes at 37°C and analyzed by flow cytometry as outlined above.

**Reagents for flow cytometry**

| Reagent | Provider | Cat-Nr. |
|---|---|---|
| CellRox Deep Red reagent | Molecular probes | C10422 |
| Fixable viability dye eFluor-506 | eBioscience | 65-0866-14 |
| HCS nucler mask Deep Red stain | Molecular probes | H10294 |
| H2-DCFDA | Molecular probes | D399 |
| Hoechst 3342 | Molecular probes | H3570 |
| Fluorometric Intracellular Ros Kit | Merck Milllipore | MAK-142-IKT |
| LYNX Rapid RPE-Cy7 antibody conjugation | BioRad | LNK111PECY7 |
| LYNX Rapid antibody conjugation kit | BioRad | LNK021RPE |
| MitoSox Red | Molecular probes | M36008 |
| MitoLite-blue FX490 | AAT Bioquest | ABD-22674 |
| MitoSpy green | BioLegend | 424805 |
| Propidium iodide | Merck Milllipore | P4864 |
| Rainbow calibration particle | BioLegend | 422903 |
| ROSstar550 | Li-Cor | 926-20000 |

| | | |
|---|---|---|
| ROSstar800CW | Li-Cor | 926-80000 |

**Statistical analysis**

Data-distribution was presented by mean-values and standard deviation of the mean; numbers of independent experiments or individual animals was indicated in the figures, legends or in the manuscript text. Student's *t*, one-way/ two-way ANOVA with Tukey post-hoc test or ANOVA with Bonferroni correction were used as indicated; in survival experiments, Kaplan–Meier curves were used and Log-rank (Mantel-Cox) test was applied to determine statistical significance; primary endpoint was development of neurological symptoms clearly indicative of hGSC. P values are indicated as *$p<0.05$, **$p<0.005$, and ***$p<0.0005$ in all results. All statistical analyses were conducted using Graph Pad Prism 5.

**Table: Software for data analysis**

| Software | Provider / citation | Application |
|---|---|---|
| Axiovision Rel 4.8 | Zeiss | Image acquisition |
| bcl2Fastq 2.15.04 | Illumina | Sequencing data analysis |
| BD coherent connection | BD Biosciences | Flow cytometry |
| BD FacsDiva | BD Biosciences | Flow cytometry |
| https://www.cbioportal.org/ | Cancer Discov. 2012, 2(5):401-4.<br>Sci Signal. 2013, 6(269):pl1. | Data mining |

| | | |
|---|---|---|
| http://www.chilibot.net/ | BMC Bioinformatics. 2004, 5:147 | Data mining |
| CLC Genomics Workbench 9.5.3 | Qiagen | Sequencing data analysis |
| CLC Sequence Viewer 8 | Qiagen | Visualization / design of genetic code |
| http://designstudio.illumina.com/ | Illumina | Visualization / design of genetic code |
| FCS Express 5 | DeNovo Software | Flow cytometry |
| FlowJo | FlowJo | Flow cytometry |
| http://gliovis.bioinfo.cnio.es/ | Neuro Oncol. 2017, 19(1):139-141. | Data mining |
| Graph Pad Prism 5 | GraphPad Software | Statistics |
| https://imagej.net/Fiji | Nature Methods. 2012, 9: 676–682 | Image processing |
| SoftMax Pro | Molecular Devices | Microplate reader |
| Tecan i-Control | Tecan | Microplate reader |
| ViiA7™ software | ThermoFischer | Analysis of qPCR data |

**Supplementary Table 1, Genes identified in pharmacogenomics screen**

| Gene-symbol | Protein-name and related information |
|---|---|
| Aimp1 | Aminoacyl tRNA synthase complex-interacting multifunctional protein 1 (EMAP-II protein; EMAP-II facilitates TNF-R1 apoptotic signalling in endothelial cells and induces TRADD mobilization. Apoptosis. 2006;11(12):2137-45) |
| Ikbkb | Inhibitor of nuclear factor kappa-B kinase subunit beta (IKKB protein; Nuclear factor-κB in Glioblastoma: Insights Into Regulators and Targeted Therapy Neuro Oncol. 2016 ;18(3):329-39) |
| Secisbp2l | Selenocysteine insertion sequence-binding protein 2-like (can substitute SECISBP2; The RNA-binding protein Secisbp2 differentially modulates UGA codon reassignment and RNA decay, Nucleic Acids Res. 2017; 45(7): 4094–4107) |
| Hnrnph | Heterogeneous nuclear ribonucleoprotein H (EMBO J. 2011;30(19):4084-97. Splicing Factor hnRNPH Drives an Oncogenic Splicing Switch in Gliomas) |
| Gm4952 | Glycine N-acyltransferase-like protein; mitochondrial acyltransferase which transfers the acyl group to the N-terminus of glycine (no specific records in PubMed; related records: New insights into the catalytic mechanism of human glycine N-acyltransferase. J Biochem Mol Toxicol. 2017;31(11) doi: 10.1002/jbt.21963) |
| Klhl17 | Kelch-like protein 17 (Actinfilin Is a Cul3 Substrate Adaptor, Linking GluR6 Kainate Receptor Subunits to the Ubiquitin-Proteasome Pathway; J Biol Chem. 2006;281(52):40164-73) |
| Clint1 | Clathrin interactor 1 (The ENTH domain protein Clint1 is required for epidermal homeostasis in zebrafish; Development. 2009;136(15):2591-600.) |
| Desi1 | Desumoylating isopeptidase 1 (DeSUMOylating isopeptidase: a second class of SUMO protease; EMBO Rep. 2012;13(4):339-46) |

## Supplementary Table 2. Characterization of primary cell-cultures from human GBM biopsies

| Code | Diagnosis | Sample-ID for genetic / genomic information | IDH WT/MUT | Primary / Recurrent | Treatment | GBM subtype (of parental tumor) | Tumorigenic in vivo | Stem-like characteristics | Patient-gender | Citation |
|---|---|---|---|---|---|---|---|---|---|---|
| GBM10 | GBM | 16073_0002 | R172H | Primary | Surgery | N.A. | N.D. | Yes | F | Cell Death Dis. 2016 Apr 28;7:e2209. |
| GBM13 | GBM | 16073_0001 | WT | Primary | Surgery | Proneural | Yes | Yes | F | Cancer Res. 2019 May 1;79(9):2298-2313. |
| GBM14 | GBM | N.D. | WT | Primary | Surgery | Mixed | Yes | Yes | M | Cancer Res. 2019 May 1;79(9):2298-2313. |
| GBM20 | GBM | 16073_0004 | WT | Primary | Surgery | Mesenchymal | Yes | N.D. | F | This study |
| GBM29 | GBM | 16073_0005 | WT | Recurrent (from patient with GBM20) | Surgery | Mesenchymal | Yes | N.D. | F | This study |
| Line2 | GBM | 16073_0015 | WT | Primary | Surgery | Classical | Yes | Yes | M | Cancer Res. 2017 Feb 15;77(4):996-1007 |
| Line6 | GBM | 16073_0017 | WT | Primary | Surgery | Mesenchymal | Yes | Yes | F | Cancer Res. 2017 Feb 15;77(4):996-1008 |
| Line7 | GBM | 16073_0018 | WT | Primary | Surgery | Proneural | Yes | Yes | M | Cancer Res. 2017 Feb 15;77(4):996-1009 |
| Line8 | GBM | 16073_0019 | WT | Primary | Surgery | Proneural | Yes | Yes | M | Cancer Res. 2017 Feb 15;77(4):996-1010 |
| Line9 | GBM | 16073_0020 | WT | Primary | Surgery | Proneural | Yes | Yes | F | Cancer Res. 2017 Feb 15;77(4):996-1011 |
| Line10 | GBM | 16073_0021 | WT | Primary | Surgery | Mesenchymal | Yes | Yes | M | Cancer Res. 2017 Feb 15;77(4):996-1012 |
| Line11 | GBM | 16073_0022 | WT | Primary | Surgery | Mesenchymal | Yes | Yes | M | Cancer Res. 2017 Feb 15;77(4):996-1013 |
| NCH421K | GBM | 16073_0006 | WT | Primary | Surgery | Proneural | Yes | Yes | M | Clinical Cancer Research, 16:2715-28, 2010. |
| NCH441 | GBM | 16073_0007 | WT | Primary | Surgery | Mixed | Yes | Yes | M | Cell Death Differ. 2014 Jun; 21(6): 929–940 |
| NCH588J | GBM | 16073_0008 | WT | Recurrent | Surgery + Radiation therapy | Mixed | N.D. | Yes | | J Pathol. 2014 Sep;234(1):23-33. |
| NCH592B | GBM | N.D. | WT | Recurrent | Surgery | Mixed | N.D. | Yes | | J Pathol. 2014 Sep;234(1):23-33. |
| NCH644 | GBM | 16073_0010 | WT | Primary | Surgery | Proneural | Yes | Yes | F | J Pathol. 2014 Sep;234(1):23-33. |
| NCH684 | GBM | 16073_0011 | WT | Primary | Surgery | N.D. | Yes | N.D. | | This study |
| BT112 | GBM | N.D. | WT | Primary | Surgery | Classical | Yes | N.D. | M | Cancer Cell. 2011 Mar 8;19(3):359-71 |
| BT172 | GBM | N.D. | WT | Primary | Surgery | Classical | Yes | N.D. | F | Clin Cancer Res. 2016 Mar 1;22(5):1185-96 |
| BT423 | GBM | N.D. | WT | Primary | Surgery | Mesenchymal | N.D. | N.D. | M | This study |

## Supplementary Table 3: Biopsies from high-grade astrocytomas

| Code | Gender | Age | Diagnosis | Primary/ Recurrent |
|---|---|---|---|---|
| | | | | |
| 138 | female | 44 | astrocytoma WHO III | primary |
| 139 | female | 50 | astroglial tumor cells | recurrent |
| 140 | male | 54 | GBM | recurrent |
| 141 | male | 46 | GBM | primary |
| 142 | male | 68 | GBM | primary |
| 143 | male | 72 | GBM | primary |